APPLICATIONS AND COMPARISONS OF THE FREQUENCY DOMAIN AND THE 45° ω-FINITE DIFFERENCE MIGRATION ALGORITHMS

Heloise Bloxsom and Rick Ottolini

Abstract

To study and compare the output quality of frequency domain and 45-degree finite difference migration algorithms, two different datasets of exploration interest are examined: a "stratified earth" and a "laterally varying earth." The migration algorithms and methods are briefly reviewed. Comparisons of the stratified-earth migrations show that the constant velocity f-k and the constant velocity 45-degree monochromatic algorithm produce nearly identical results. For interpretation, the $V = V(t)$ frequency domain or the $V = V(z)$ 45-degree finite difference algorithms are more correct and produce sections of comparable quality. Migrations of the laterally varying earth show that $V = V(x,z)$ algorithms must be used, and that the velocity model dramatically affects the output picture. Two current fields of research are benefited by $V = V(x,z)$ migration algorithms: the nature of the continental crust at depth, and the correct imaging of sediments under thrust zones.

Introduction

The two different datasets examined are from COCORP's (Consortium for Continental Reflection Profiling) Wyoming Line 1. Figure 1 is the base map for the Wyoming data. Line 1 is 52.4 km in extent, 15 sec long, with a sample rate of .008 sec. The "stratified earth" data is a 384-trace, 750-timepoint (6 sec) segment of line 1, in the Green River Basin. (See Figure 2.) To a first order approximation, one velocity function $[V = V(t)]$ can be used for this dataset. The "laterally varying earth" data is a 320-trace, 750-timepoint segment of line 1 over the Wind River thrust in Wyoming. (See Figure 3.) The thrust outcrops at the surface at trace 43 (Figure 3); to the left of the thrust are the Green River Basin sediments; to the right, Precambrian rocks have been thrust over the layered sediments. A velocity model $[V = V(x,z)]$ must be used to describe this dataset.

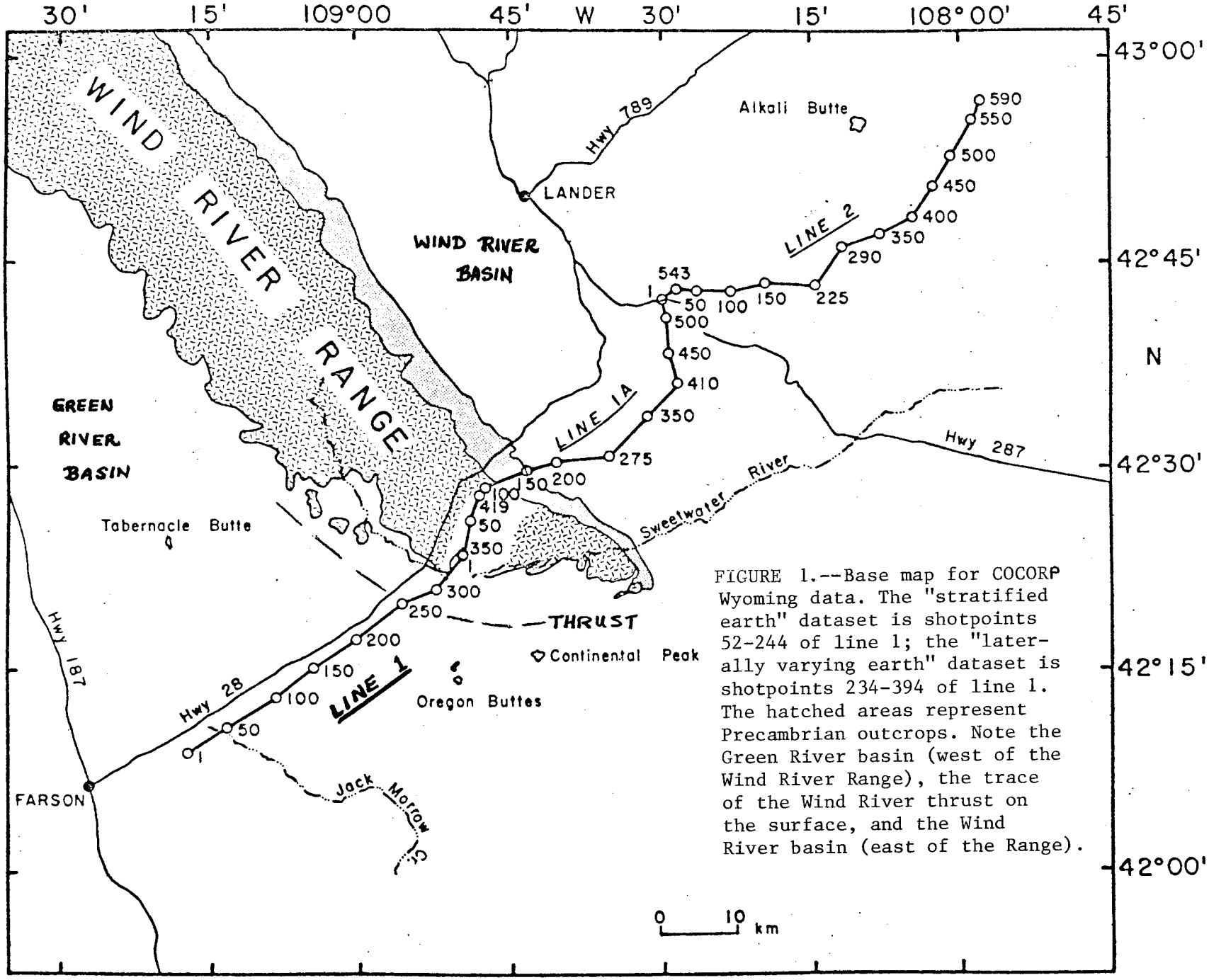

FIGURE 1.--Base map for COCORP Wyoming data. The "stratified earth" dataset is shotpoints 52-244 of line 1; the "laterally varying earth" dataset is shotpoints 234-394 of line 1. The hatched areas represent Precambrian outcrops. Note the Green River basin (west of the Wind River Range), the trace of the Wind River thrust on the surface, and the Wind River basin (east of the Range).

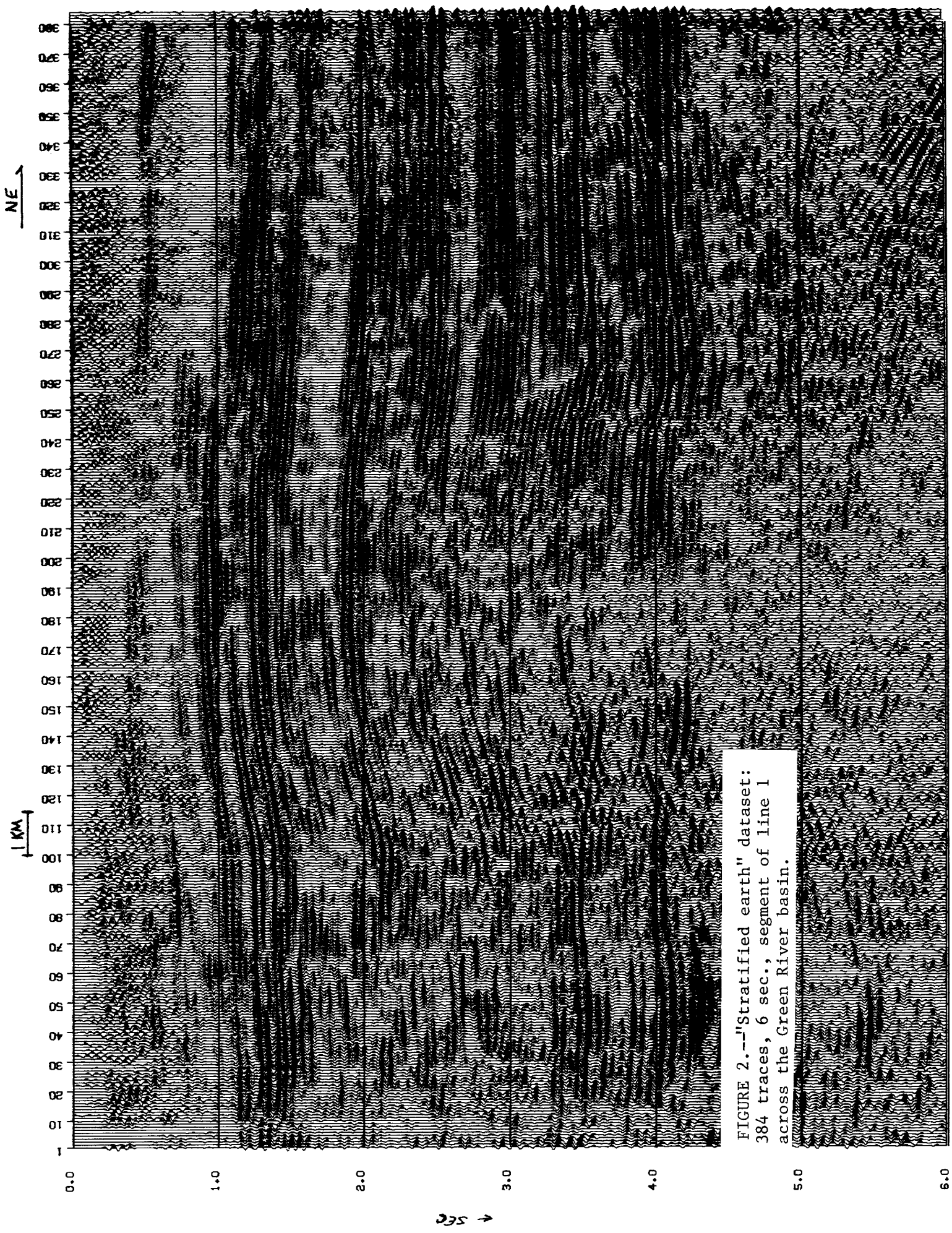

FIGURE 2.--"Stratified earth" dataset: 384 traces, 6 sec., segment of line 1 across the Green River basin.

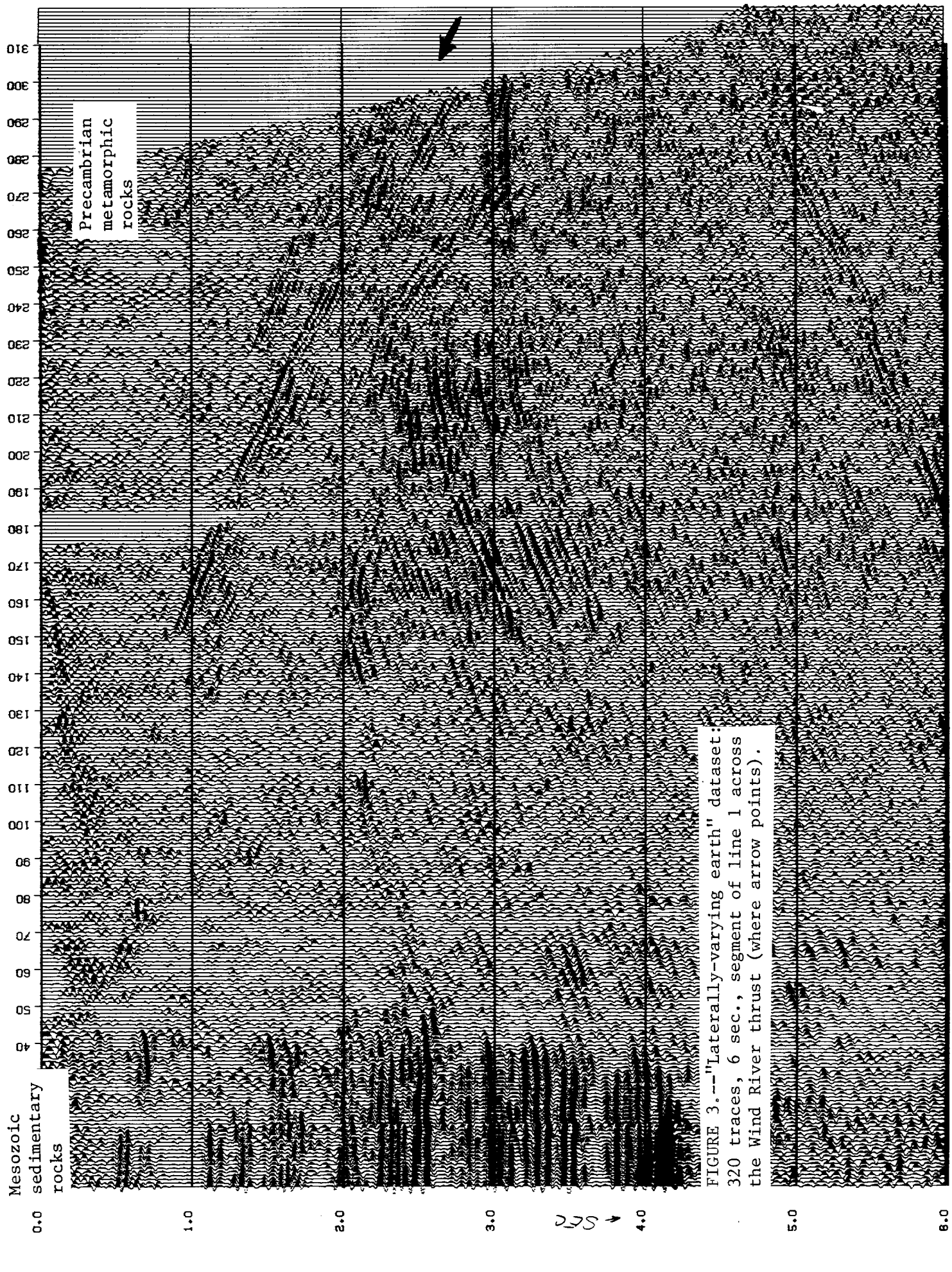

FIGURE 3.--"Laterally-varying earth" dataset: 320 traces, 6 sec., segment of line 1 across the Wind River thrust (where arrow points).

Review of migration algorithms and methods

Our frequency domain algorithm is from Stolt (1978, Equation 50):

$$A_{mig}(k_x,\omega') = vk_z(k_x^2 + k_z^2)^{-1/2} \; A_{dif}\,[k_x,\omega=v(k_x^2 + k_z^2)^{1/2}] \qquad (1)$$

where A is the Fourier transformed data, A_{mig} = A migrated, A_{dif} = A diffracted, and ω, ω' are the unmigrated and migrated time frequencies. This equation is a frequency domain solution to the two-dimensional acoustic wave equation. It says that the two-dimensional Fourier transform of the migrated time section is a simple mapping and rescaling of the two-dimensional Fourier transform of the data. Such a vector-oriented equation is easy to implement on a mini-computer and is facilitated by the use of an array processor. Frequency domain methods need only two points/wavelength, not the eight points/wavelength of the finite difference methods, and are limited to constant velocity models.

An extension to Stolt's algorithm (Stolt, 1978, Equation 75) handles variable velocities in a limited way by a pre- and post-migration stretching of the data to and from a pseudo-depth domain. The coordinate transformation is

$$d = \left\{ 2 \int_0^t [V_{rms}(t)]^2 \, t \, dt \right\}^{1/2} \qquad (2)$$

where d is the pseudo-depth axis. Seismic data may appear "depth-shortened" (due to higher velocities deeper), which can be likened to the visual illusion of the "near" bottom of a pool of water. Physically, the pseudo-depth transformation is a compensation for this apparent depth-shortening. Geometrically, an increasing velocity gradient flattens the tops of diffraction hyperbolae. The pseudo-depth transformation moves the hyperbola to a position where its apex curvature resembles a constant velocity case. This algorithm is inaccurate for high dips because the stretch cannot compensate for crossing hyperbola limbs in variable velocity media. This algorithm makes no allowances for lateral velocity variation. Stolt's algorithms try to collapse hyperbolae to their apexes, whereas an off-apex position is correct in the presence of lateral velocity variations.

The third migration method is a 45-degree ω-finite difference algorithm which uses an equation derived by Kjartansson (see p. , this report):

$$\frac{i}{2\bar{m}} Q_{xxz} + Q_{xx} + 2\, i\, \bar{m}\, Q_z + \frac{i}{2\bar{m}} (m^2 - m^{-2}) Q_z +$$

$$(m^2 - m^{-2}) Q + \frac{im}{\bar{m}} \frac{dm}{dz} Q = 0 \qquad (3)$$

The data is Fourier transformed over time, then transposed (into strips of x). The monochromatic 45-degree wave equation is then run at each z-level for a suite of frequencies (usually up to three-quarters of the Nyquist frequency). Summing over the real part of the frequencies used yields the answer at that z-level. The velocity model is given in z (depth) and interval velocity: the model may be constant velocity, or depth-variable (the program linearly interpolates between user-given z-velocity pairs), or depth-and-laterally-variable. (See Kjartansson, p. this report.)

After the frequency domain migrations, we usually apply a migration gain correction. We all know that migration is equivalent to collapsing a hypothetical diffraction hyperbola to a (migrated) output point. On very deep seismic sections (10-15 sec two-way traveltime), however, there are noticeable hyperbola truncation energy losses near the lower section boundaries. A migration gain correction normalizes the partial hyperbola to the strength of a full hyperbola everywhere on the section. The normalization formula is

$$n = \Delta x_\ell (\Delta x^2 + v^2 t^2)^{-1/2} + \Delta x_r (\Delta x_r^2 + v^2 t^2)^{-1/2} \qquad (4)$$

where the point scatterer is at (x,t) and Δx_ℓ and Δx_r are distances from the (left and right) sides of the section. This equation comes from integrating the amplitude along a hyperbola. The amplitude of a point scatterer diffraction as a function of observation angle from the vertical is given by:

$$a(\theta) = \cos\theta = z(\Delta x^2 + z^2)^{-1/2} \qquad \theta < \left(-\frac{\pi}{2}, +\frac{\pi}{2}\right) \qquad (5)$$

On our deep migrated sections (15 sec record length), an energy "dropoff" at 11 to 12 sec is often observed both before and after the migration gain correction has been applied. Therefore, the dropoff is probably not a processing artifact.

A stratified earth

Figures 4, 5, and 6 are the migrated stratified earth sections. Figure 4 is a frequency domain constant velocity migration at 13,100 ft/sec (3.99 km/sec). This velocity was chosen to focus the syncline at 3.5 sec. Figure 5 shows a 45-degree ω-finite difference constant velocity migration at 13,100 ft/sec. Figure 6 is a Stolt stretch frequency domain migration [V = V(t)], where the velocity function was chosen by analyzing the velocity scans. Note that the Pacific Creek anticline is in the center of this dataset. Strictly speaking, because of the anticline, there are small lateral velocity variations; but (a) these variations are second order, and (b) if there were no dips at all, migration would not be needed and the effects of migration would be imperceptible. The unmigrated syncline at depth (3.5 sec) has the classic "bowtie" appearance. All three migrations focused this event. The steeply dipping energy at 5.8 to 6.0 sec on the unmigrated data is seen at 5 to 5.5 sec on the frequency domain migrations; it is not seen on the 45-degree migration because 50 fewer time samples were (inadvertently) input into the run. The test posed by this data, however, is to focus the syncline.

The interference patterns seen in the events at 3.8 to 4.2 sec on the right edge of the sections are probably due to the laterally varying velocities just to the right of the section (the adjacent thrust fault).

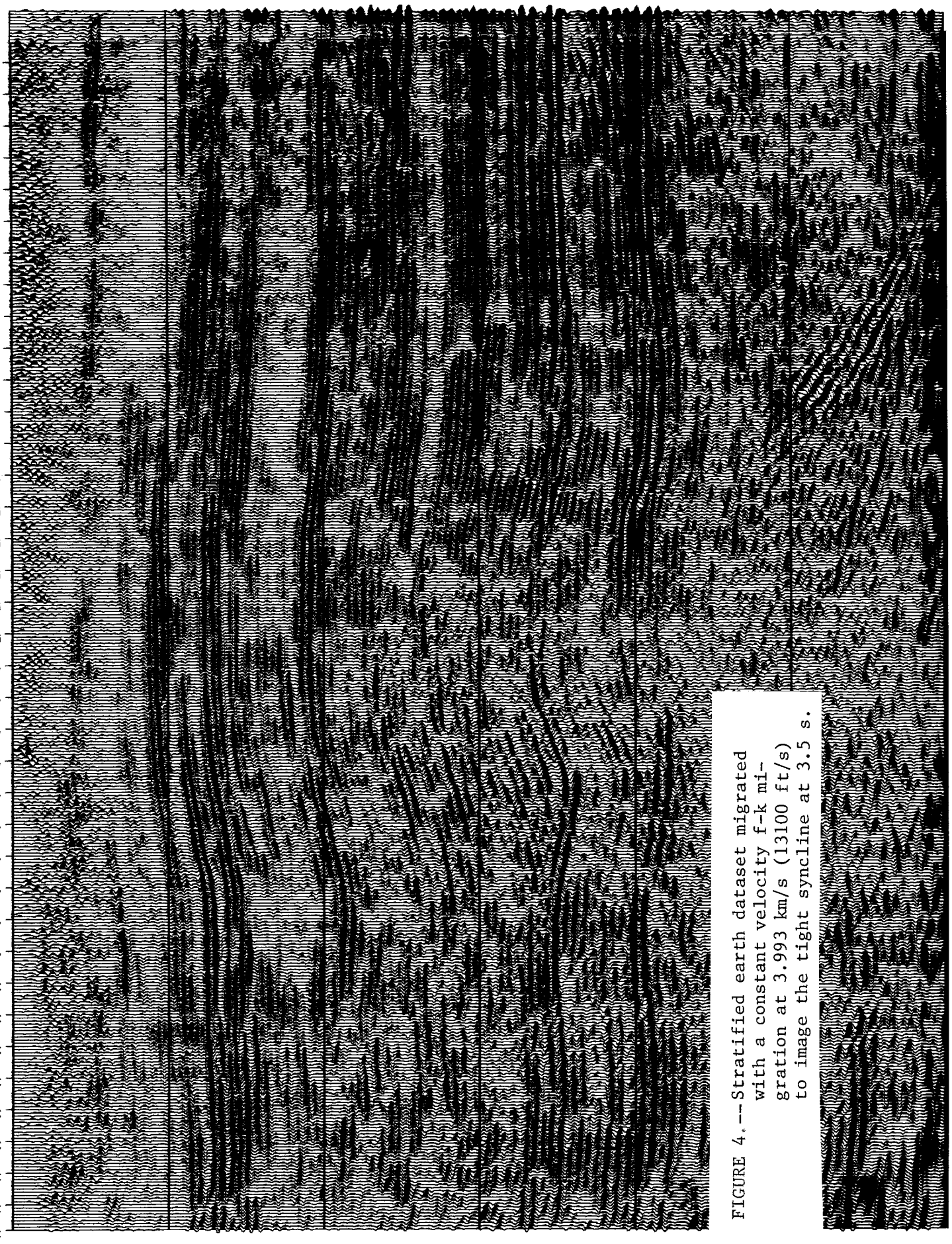

FIGURE 4.--Stratified earth dataset migrated with a constant velocity f-k migration at 3.993 km/s (13100 ft/s) to image the tight syncline at 3.5 s.

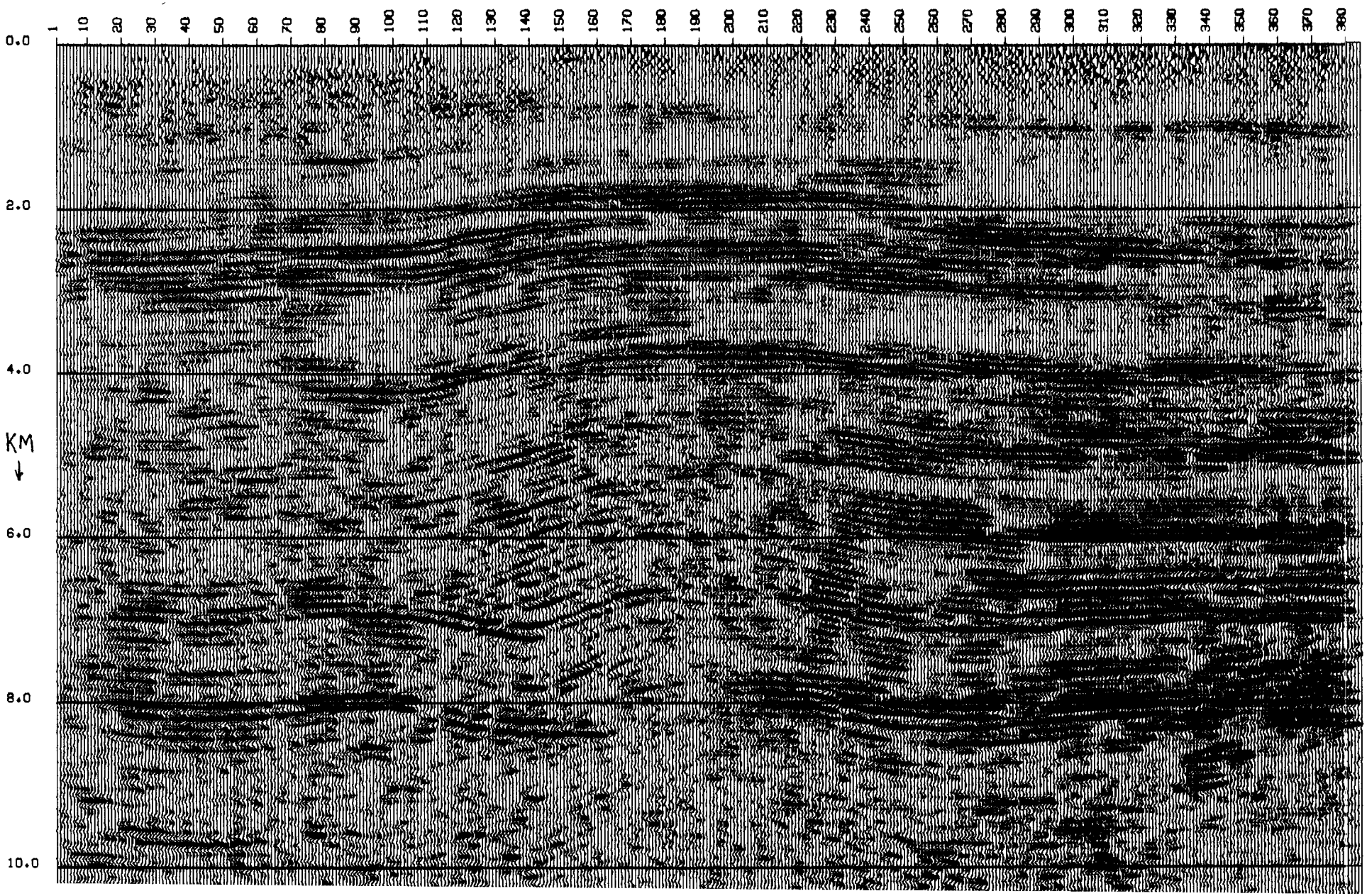

FIGURE 5.--Stratified earth datset migrated with a 45° ω-finite difference constant velocity (3.993 km/sec). In the stratified media case, the constant velocity f-k and the constant velocity 45° finite difference algorithms produced nearly identical results.

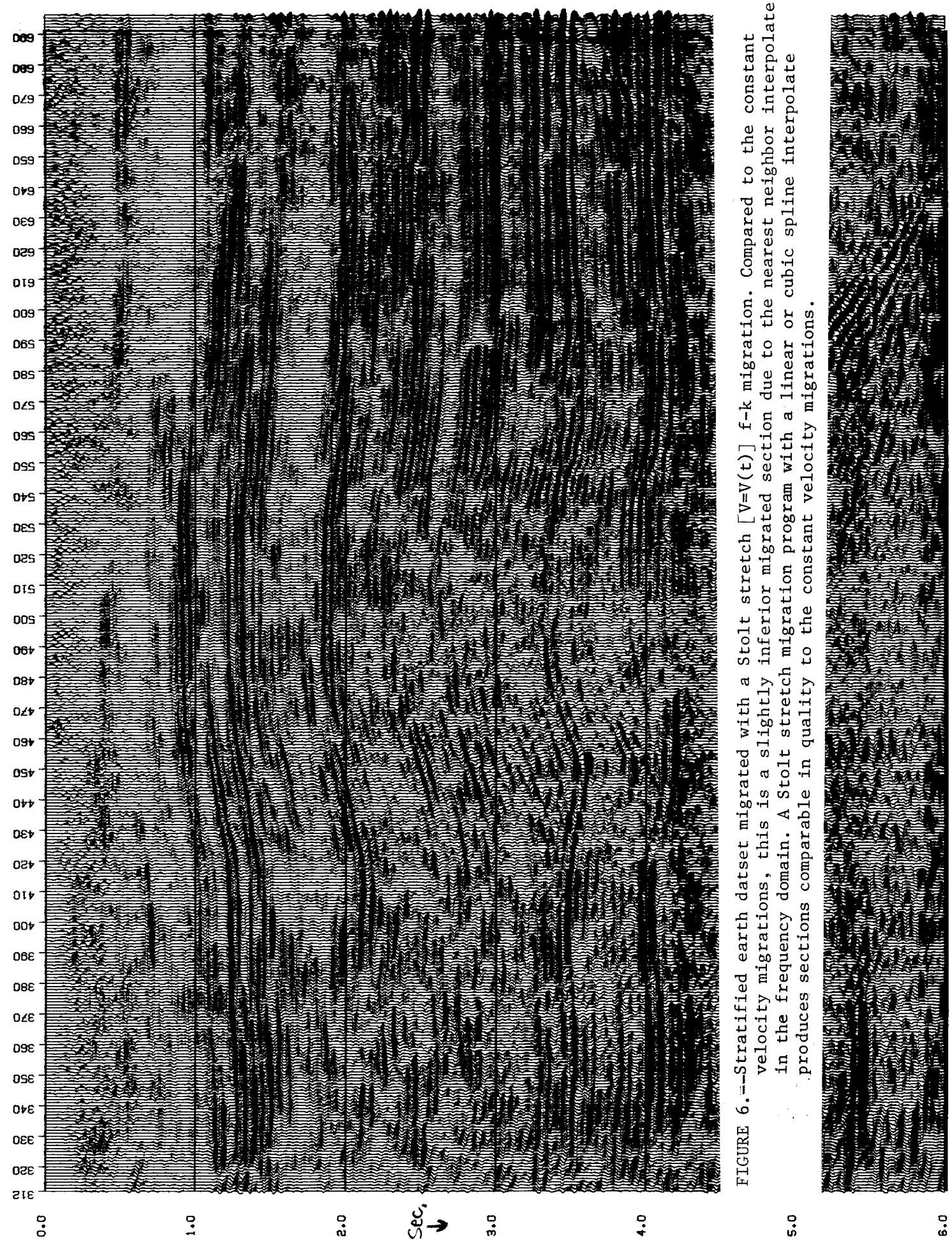

FIGURE 6.—Stratified earth datset migrated with a Stolt stretch [V=V(t)] f-k migration. Compared to the constant velocity migrations, this is a slightly inferior migrated section due to the nearest neighbor interpolate in the frequency domain. A Stolt stretch migration program with a linear or cubic spline interpolate produces sections comparable in quality to the constant velocity migrations.

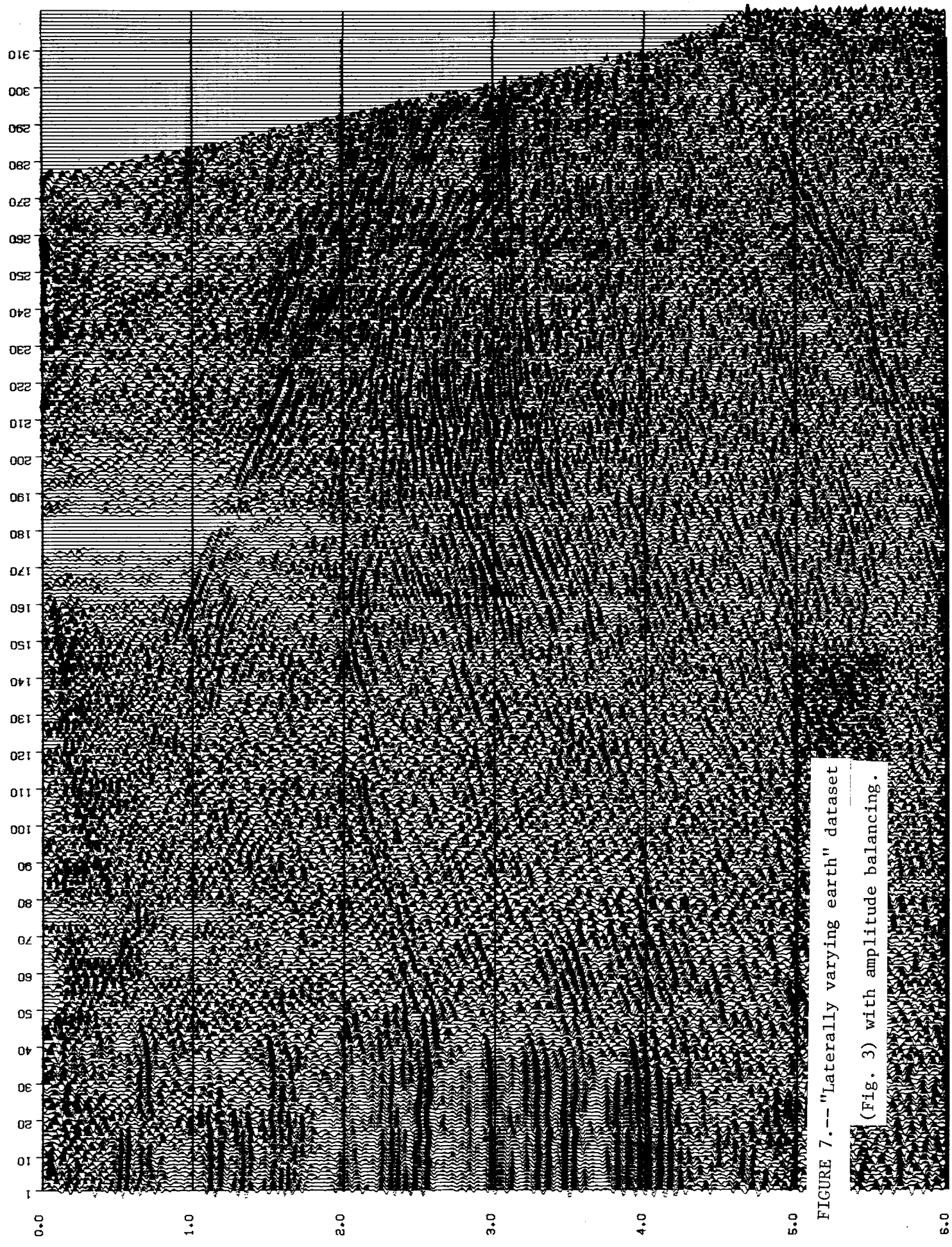

FIGURE 7.--"Laterally varying earth" dataset (Fig. 3) with amplitude balancing.

Conclusions. In the stratified media case we have found that our constant velocity f-k and the constant velocity 45-degree finite difference algorithms produced nearly identical results. The Stolt stretch [V = V(z)] algorithm, although very quick and inexpensive, produces a slightly inferior migrated section due to the nearest neighbor interpolate in the frequency domain. A Stolt stretch migration program with a linear or cubic spline interpolate produces sections comparable in quality to the constant velocity migrations.

A lateral velocity varying earth

The input dataset is shown in Figure 3. A lateral amplitude balancing program was run on the data in order to increase the amplitudes between trace 50 and trace 140. The balancing program looks within user-specified windows across the data (in the x-direction) and calculates an average value within the window for each trace. The data is then scaled such that the average value is the same for each trace within each window. The scaling factor is linearly interpolated down each trace (in time) between the windows. [The parameters used to make Figure 7 were: (.5 sec, 1.0 sec, 1.0 av. value), (2.0, 3.5, 1.0), (4.5, 5.5, 1.0).] As is immediately obvious, the program did not work very well in the area of the skip zone. The quality of the thrust reflection has deteriorated. Our goal was to enhance the "dead zone" between traces 50 and 140, however, and this was achieved.

These two sections (the unbalanced and balanced) were input to Kjartansson's 45-degree [V = V(z,x)] ω-finite difference program. The velocity-earth model is specified in z (depth) and interval velocity. Two basic models were used: a linear thrust zone, and a nonlinear thrust zone (based upon the seismic expression of the thrust). Figure 8 shows the models used.

A 45-degree ω-finite difference algorithm with V = V(z,x) was used to produce Figures 9 through 13. Figures 9 and 10 show the unbalanced section (Figure 3) migrated with a nonlinear and a linear thrust model (respectively). Note the difference in the continuity of the sediments at the left edge of the section. Figure 9 has northeasterly dipping energy at 5.6 km depth and the clearly defined sediments cease about trace 43. Figure 10 has no

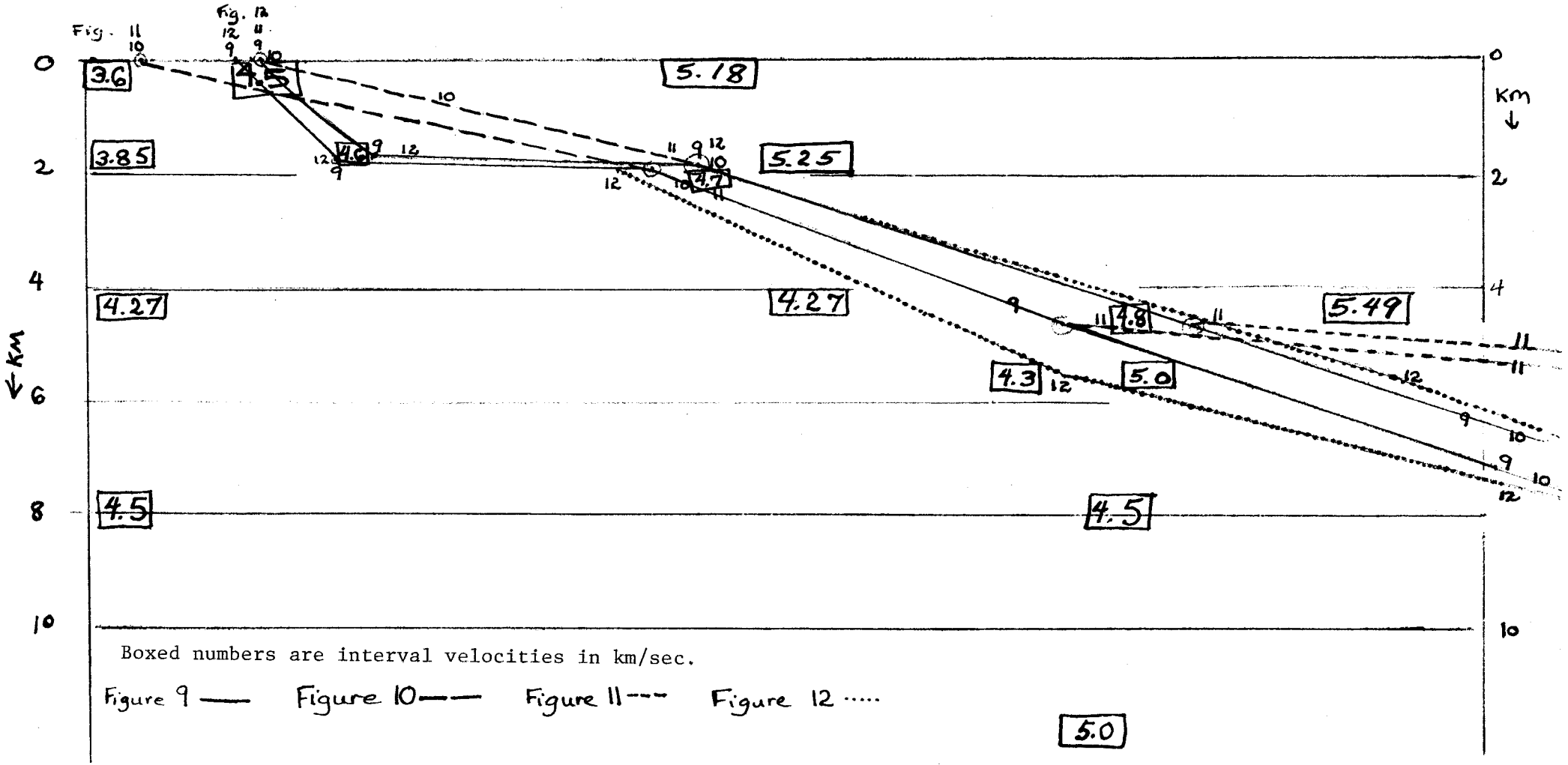

FIGURE 8.— The velocity models [V=V(x,z)] used. Note the two types of model: a non-linear thrust zone (Figures 9 and 12) and a linear thrust zone (Figures 10 and 11). The nonlinear thrust model was based on an interpretation of the preliminary migrations; the linear thrust model is a simpler approximation/guess concerning the nature of the subsurface. The velocities are based on petrologic and geologic knowledge, not seismic interval velocities. (Migrations of this dataset using seismic interval velocities are seen in Bloxsom and Kjartansson's paper, this SEP report.)

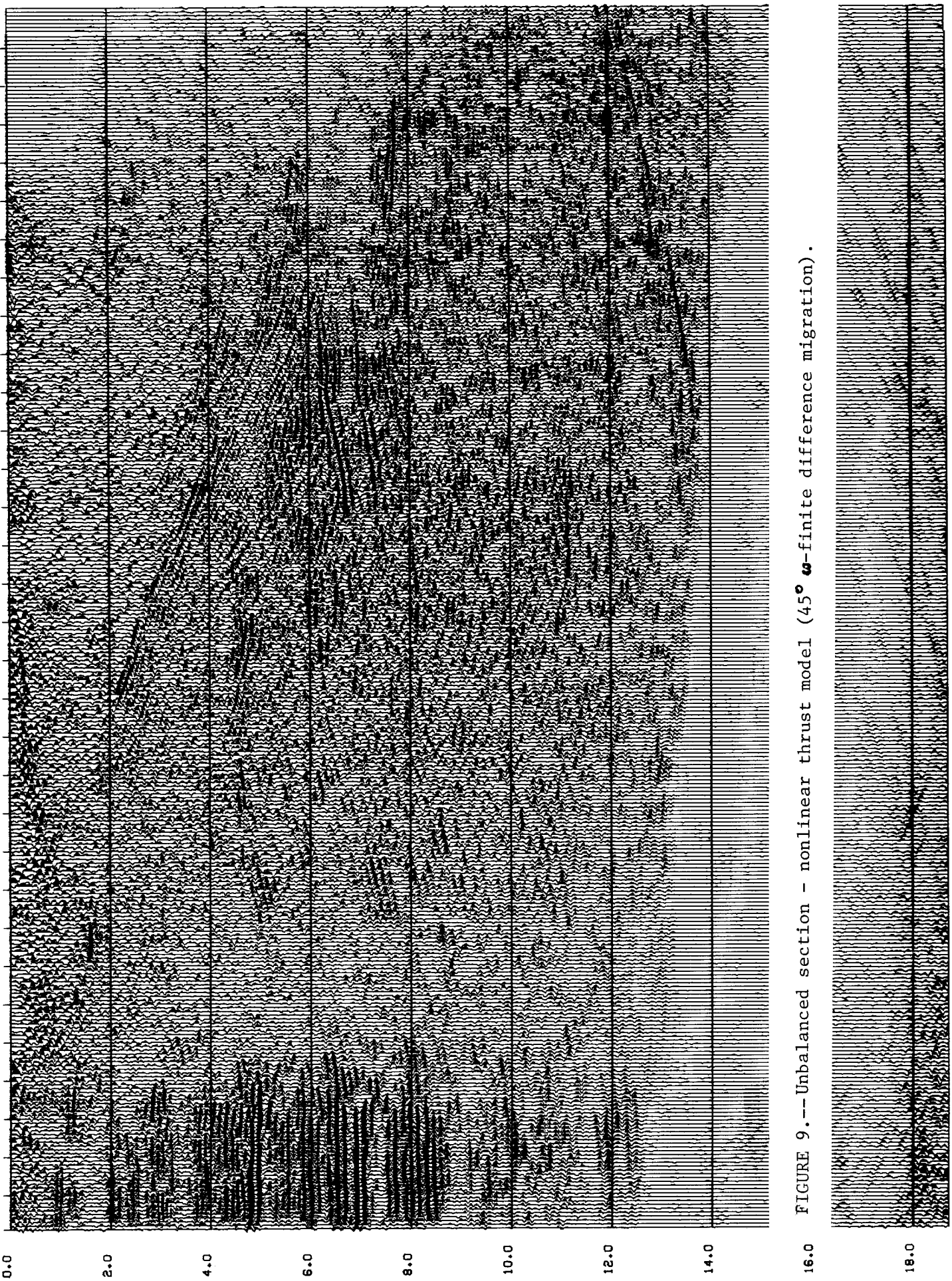

FIGURE 9.--Unbalanced section - nonlinear thrust model (45° ω-finite difference migration).

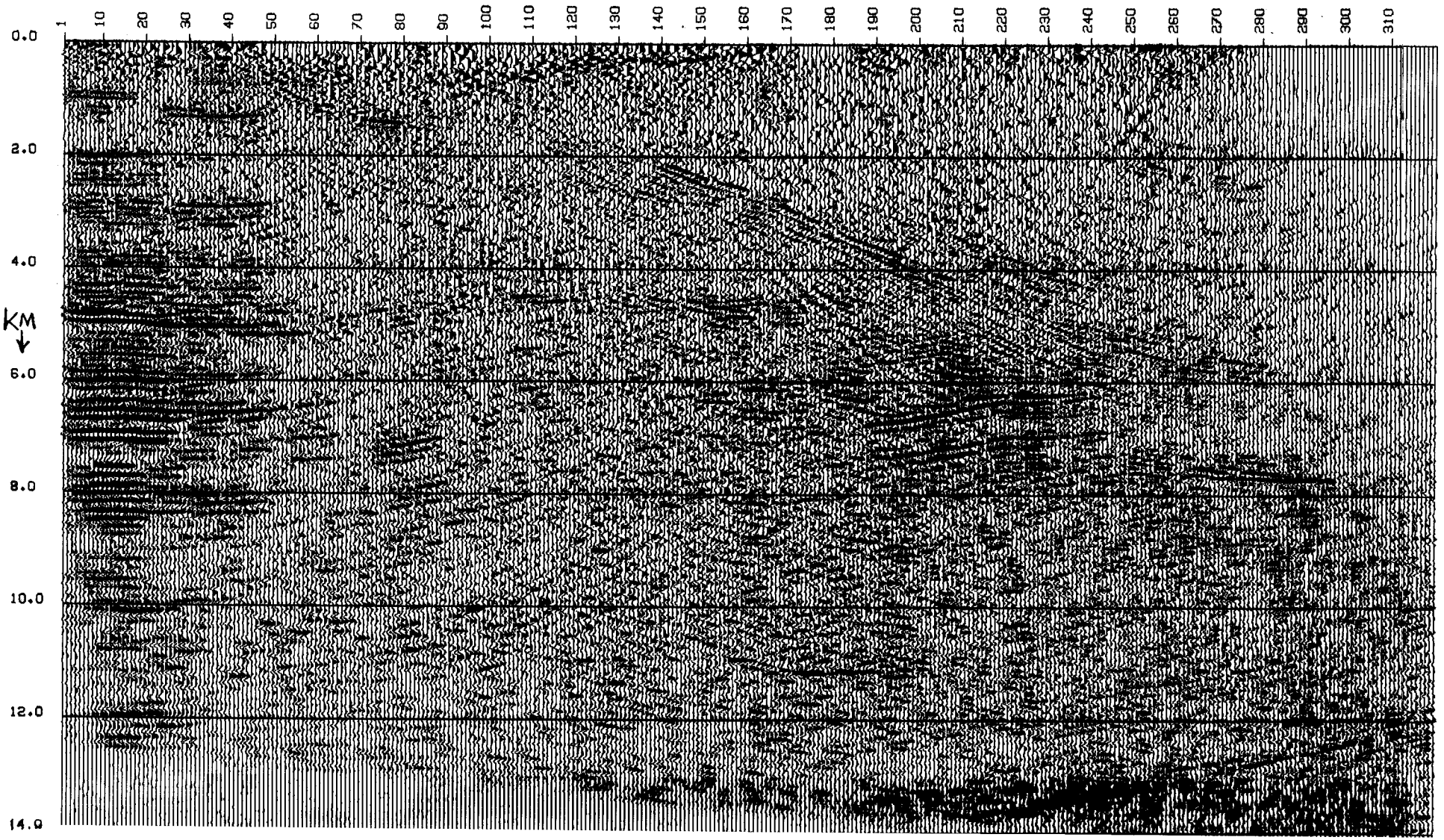

FIGURE 10.--Unbalanced section input. Linear thrust model (45° migration). The model used dramatically affects the output. Compare continuity of events around 5 km from trace 40 to trace 110. Compare event dipping to the right at 5.5 km traces 30-40 on Fig. 9 with absence of that event on Figure 10.

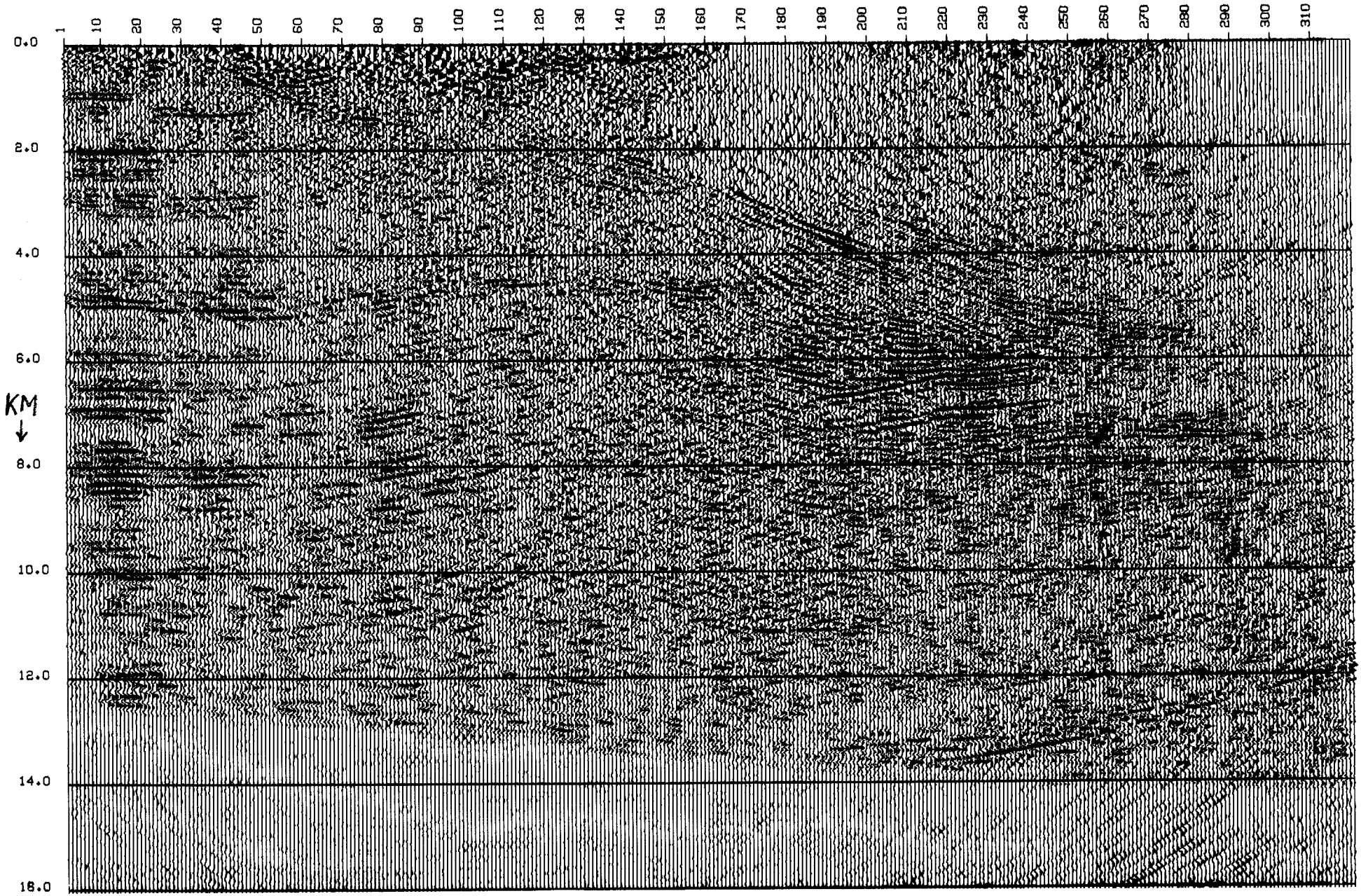

FIGURE 11.--Balanced section - linear thrust model (45° migration).

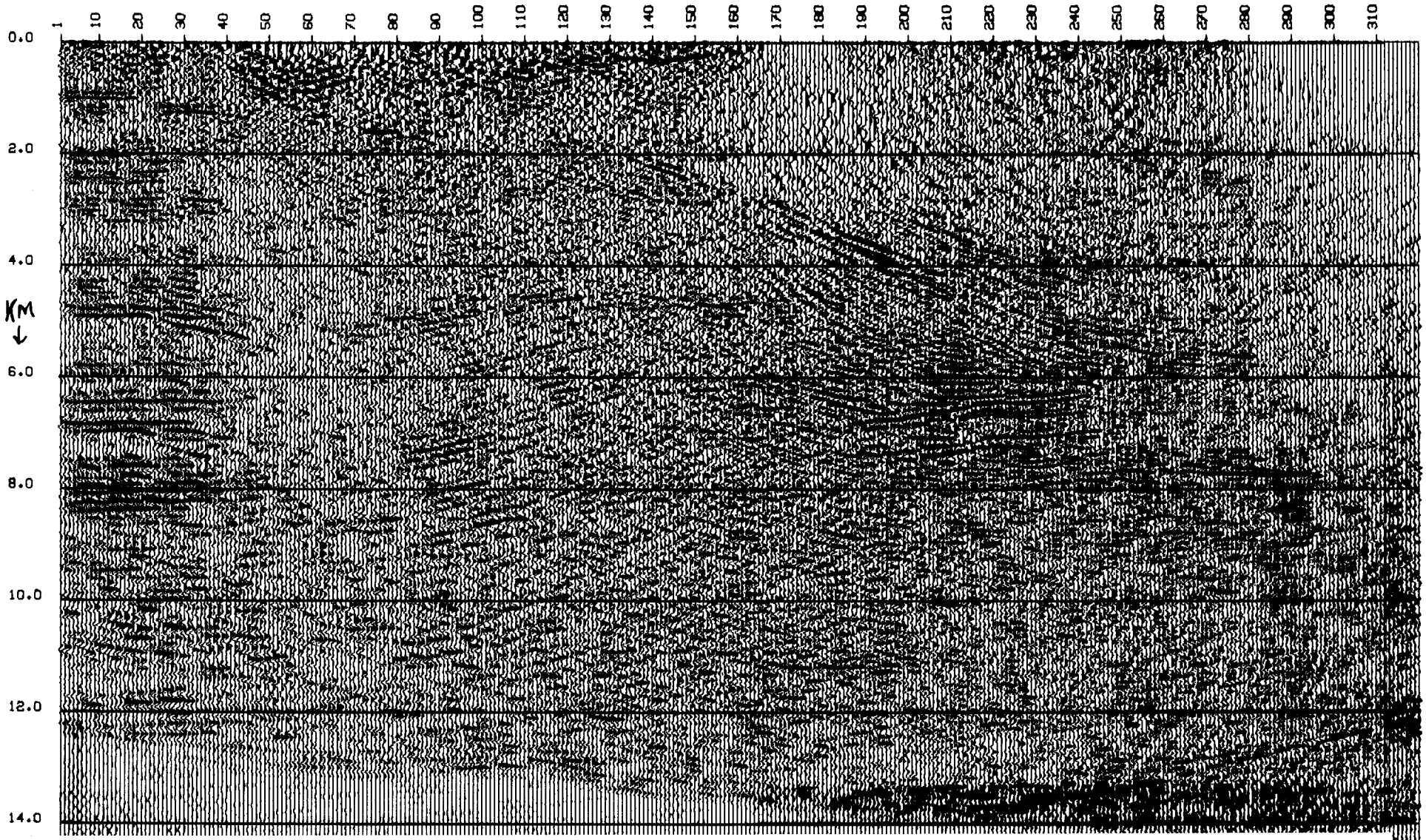

FIGURE 12.--Balanced section - nonlinear thrust model (45° migration). The spatial distribution of the amplitude strengths affects the output quality: compare Fig.s 9 and 12; Fig.s 10 and 11. The balanced section input created better migrations between traces 30 and 100; the unbalanced sections created better migrations of the thrust zone between traces 120 and 250. Note the strong event dipping to the left on Fig. 12 at around 5.3 km, traces 20-50; note its absence on Fig. 11.

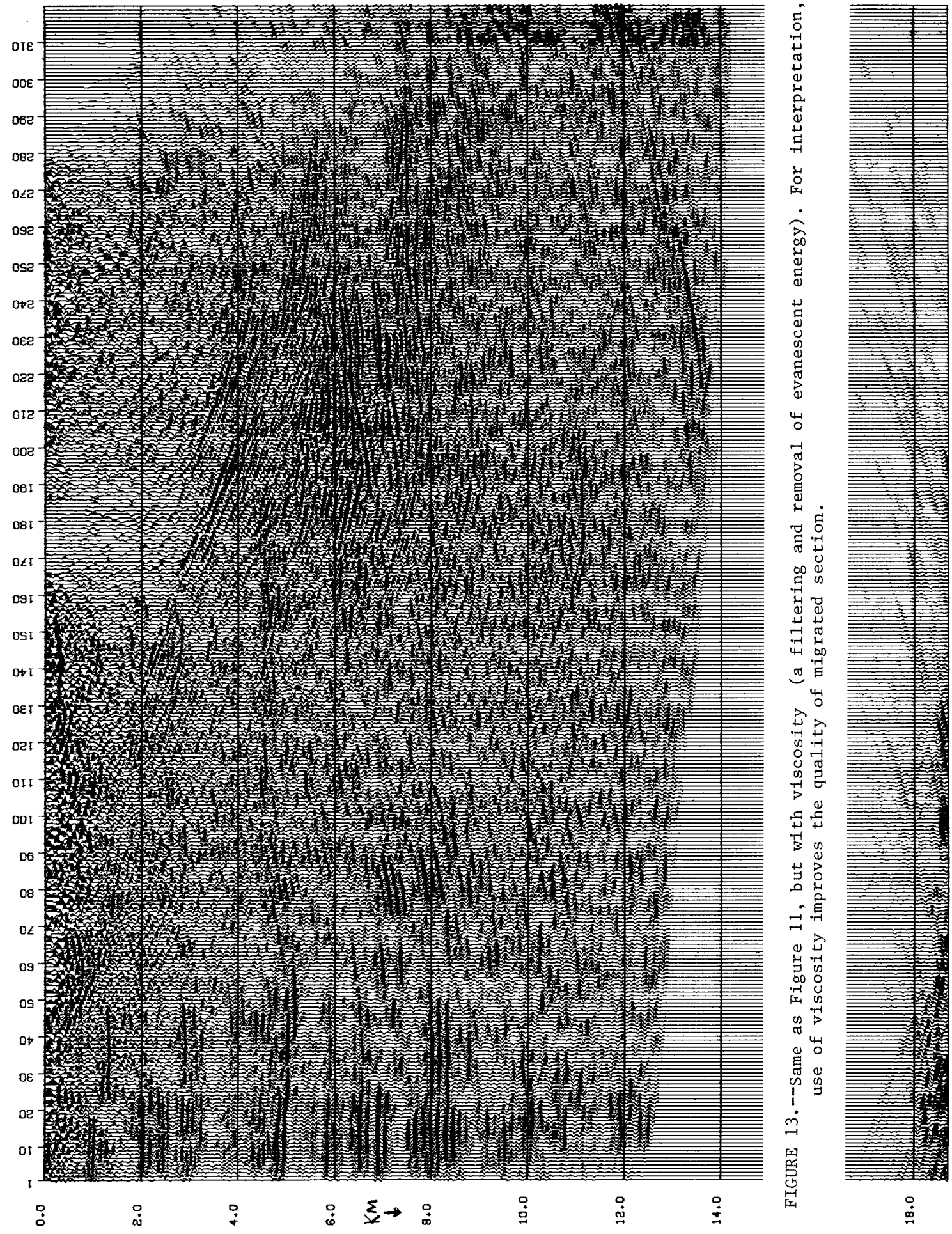

FIGURE 13.--Same as Figure 11, but with viscosity (a filtering and removal of evanescent energy). For interpretation, use of viscosity improves the quality of migrated section.

northeast dip segments interfering with the sediments' reflections, and the sediments' reflections continue out farther, to about trace 50. Also on Figure 10, the thrust fault above 2 km appears to be more clearly defined. Note that on this figure the continuity of the high amplitude reflection at 5 km is much better.

Figures 11, 12, and 13 used the amplitude-balanced data for input. Figure 11 resulted from a straight thrust model; Figure 12 from a non-linear thrust model; Figure 13 is the same migration as Figure 11, only *with* a viscosity (a removal of evanescent energy). The order of these figures permits easy comparison of Figures 9 and 11: this comparison (by flipping the page rapidly) shows how dramatically the model and the pre-migration balancing affected the ouput. (Figure 9 is a non-balanced input with a nonlinear thrust zone; Figure 11 is a balanced input with a linear thrust zone.) Figures 11 and 13 may be easily compared to see the effect of removing evanescent energy. The continuity of the sediments on the left edge of the section, the believability of the dips, and the quality of the section is much better on Figures 11 and 13 than on Figure 9.

We believe Figures 11 and 13 to be the more accurate picture of the subsurface. There is still work to be done on this dataset -- we believe that the broken (higher amplitude) reflector at 5 to 5.3 km from trace 1 to trace 160 can be more accurately imaged: we have not yet selected the optimum parameters for the migration.

Figure 14 is a frequency domain migration, with $V = V(t)$, *i.e.* a Stolt-stretch f-k migration. The input was a 500-trace, 1000-time point dataset which extended 180 traces to the left of the "laterally varying earth" dataset. The entire migrated output was 1024 traces, 1000 time points. Figure 13 is only a 320-trace, 750-time point segment corresponding to the portion under consideration. This migration algorithm makes no allowance for lateral velocity variations, and so does not correctly place energy in t and x. This section is useful, however, as a *rough* estimate of the approximate location of dipping energy after migration. The $V(t)$ function chosen is correct for the sedimentary section on the left of the section.

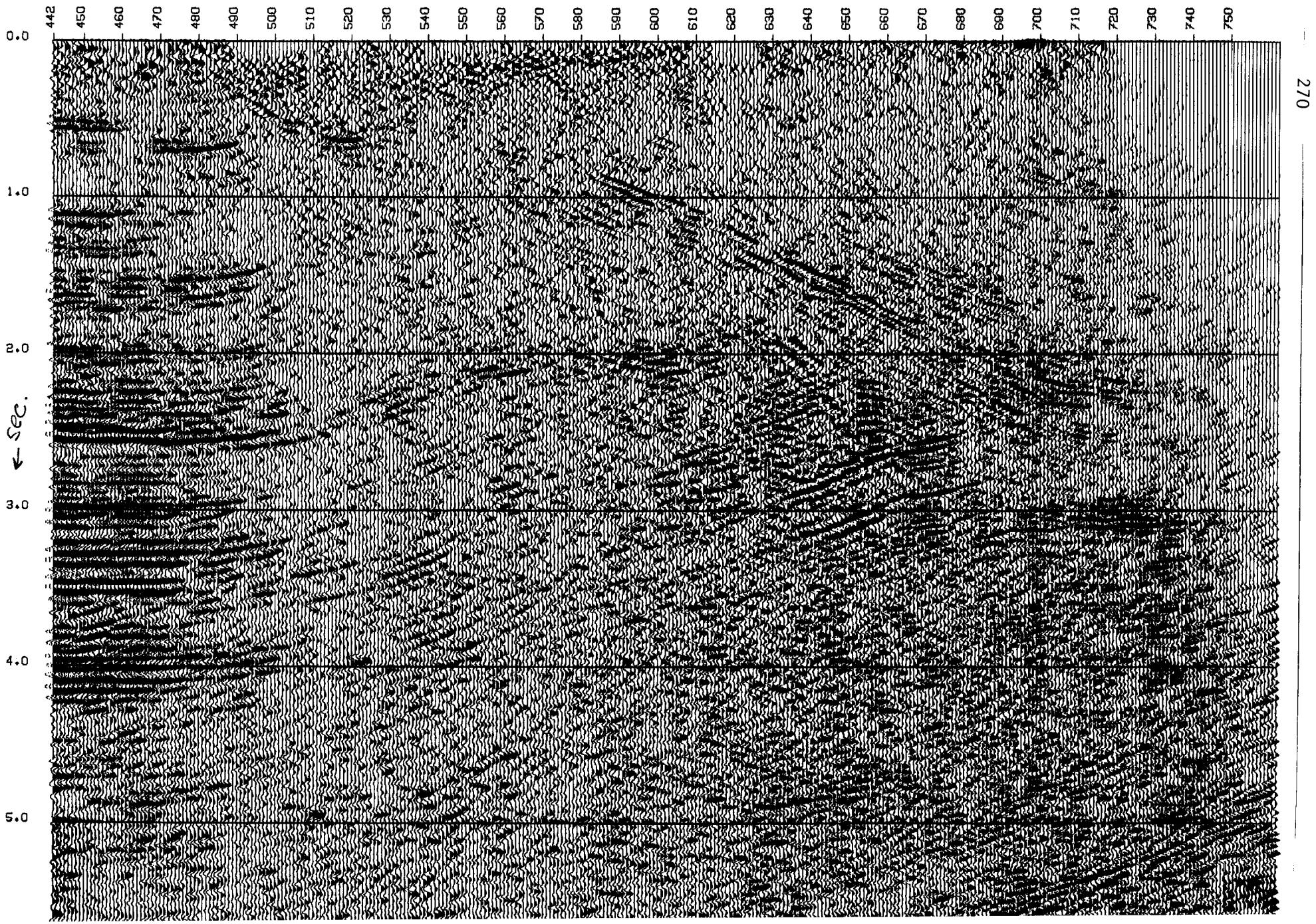

FIGURE 14.--V=V(t) Stolt stretch f-k migration. In the presence of strong lateral velocity variations, the migration algorithm must have V=V(x,z). In this migration, dipping energy was not moved to its correct lateral position. (The velocity function used was correct for the sedimentary sequence on the left.)

Conclusions

In the presence of strong lateral variations, the migration algorithm used must have $V = V(z,x)$. The model used dramatically affects the output picture. The spatial distribution of the amplitude strength affects the output quality also with respect to artifacts induced by the 45-degree algorithm. Bloxsom and Kjartansson's paper (this SEP report) shows that: (1) a velocity contrast in the model creates in the output migrated depth section an apparent higher frequency content in the lower velocity sediments (with apparently lower frequencies in the higher velocity zone); (2) interfaces dipping more than 45 degrees on real data introduce artifacts on the migration sections.

When the earth can be approximated by $V = V(t)$, we have found that constant velocity migrations using either a 45-degree finite difference algorithm or an f-k algorithm produces sections of comparable quality. For *interpretation*, however, it is necessary to use a $V = V(t)$ or $V = V(z)$ algorithm to image all depths "correctly."

Two fields of research are interwoven with this dataset and the lateral velocity variation migration algorithm: (1) to learn more about the nature of the continental crust, the deep reflection (5 to 15 sec), researchers need data properly imaged down to the Moho, even with such radical velocity variations in the "near" surface; (2) to find economic hydrocarbon accumulations in Wyoming and similar regions, the explorationists must accurately image the sediments under thrust zones. There is considerable interest here in both of the above fields.

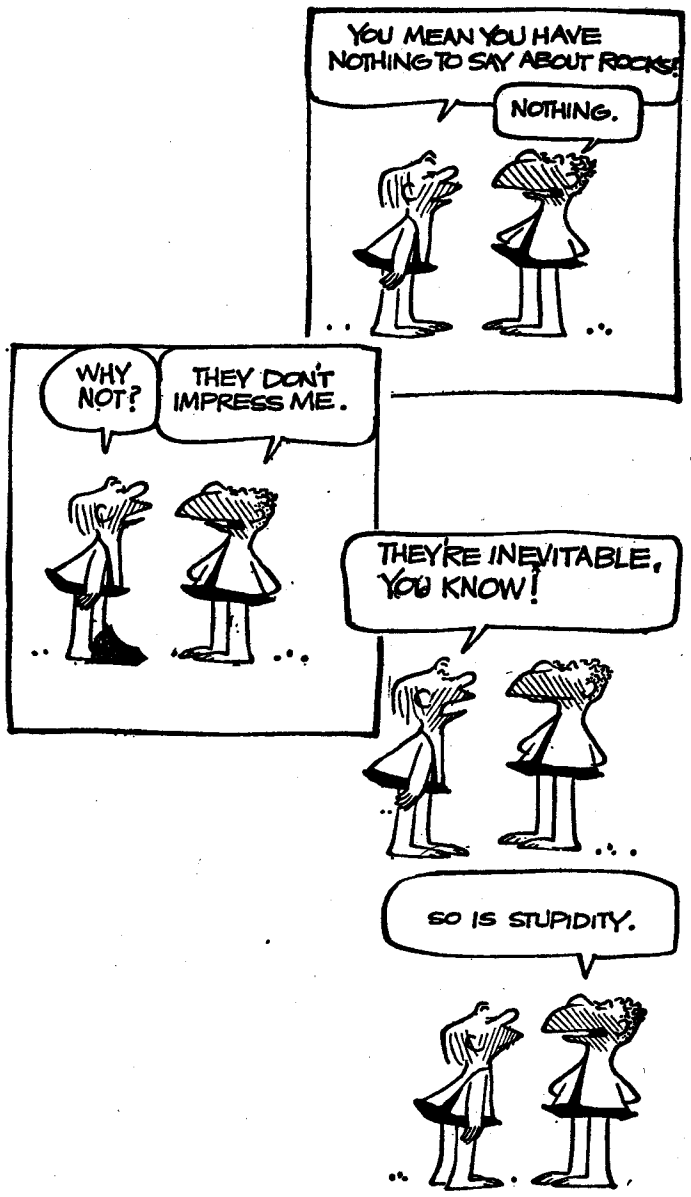
YOU MEAN YOU HAVE NOTHING TO SAY ABOUT ROCKS?
NOTHING.
WHY NOT?
THEY DON'T IMPRESS ME.
THEY'RE INEVITABLE, YOU KNOW!
SO IS STUPIDITY.